

A WEAK COUPLING METHOD BETWEEN THE DYNAMICS CODE HOST AND THE 3D UNSTEADY EULER CODE WAVES

G. Servera, P. Beaumier, M. Costes

ONERA, Applied Aerodynamics Department, Châtillon, France

Abstract

This paper presents a weak coupling method between the HOST dynamics code and the WAVES Euler aerodynamic solver for computing the trim of a flexible rotor in steady forward flight. The coupling can be applied on the lift, the pitching moment and the drag variables which are introduced as corrections to the simplified aerodynamics used in HOST. On the other hand, the blades motion and deformation are taken into account in WAVES by a deforming grid approach. Applications to the 7A and 7AD model rotors show that a simultaneous coupling on these 3 parameters is required in order to obtain a converged solution independent on the simplified aerodynamic model used in HOST. The coupled solution provides significant improvements on the pitching moment and torsion prediction, but further work is necessary to obtain an improved solution for the remaining parameters.

Introduction

An accurate computation of the flow field generated by helicopter main rotor blades requires to consider at the same time both the aerodynamic and the structural properties of the rotor. Indeed, blade motion and deformation directly arise from the trim between the aerodynamic and inertial forces applied to the blade, while, on the other hand, aerodynamic loads are strongly dependent on blade dynamics and more especially blade motion and torsional deformation.

Typical methods to solve both the dynamic and the aerodynamic aspects consist in using a simplified aerodynamic model in the dynamics computation. General equations governing the trim between inertial, elastic and aerodynamic loads are solved by computing the aerodynamics according to a 2D quasi-steady model. The blade is thus assumed to be a lifting line and sectional aerodynamic loads are generally determined by 2D analytical expressions or experimental airfoil data. Approximations for unsteady and transonic corrections may also be introduced in the loads and moments computation. Induced velocities are obtained either by linear inflow models (e.g. Meijer- Drees) or by modeling the rotor wake as a set of vortex elements of prescribed geometry.

Computation is made by coupling together the rotor wake, the aerodynamic and the dynamic solutions in order to trim the whole rotor.

Alternatively to these methods which use the classical blade element theory, one solution to predict airloads more accurately is to use Computational Fluid Dynamics (CFD) methods. Indeed, CFD codes compute the 3D transonic and unsteady flow field generated by the blades solving the Navier-Stokes, Euler or Full-Potential equations. Blades rigid motion and deformations are provided by the dynamics calculation and given as inputs in the CFD computation. However, a coupling of CFD with dynamics is necessary to account for the 3D aerodynamic field in estimating the blade motion and deformation.

In principle, the simplest way to couple 3D unsteady aerodynamics with dynamics is to replace the simplified aerodynamic model used in the dynamics by a CFD analysis. This possibility was demonstrated by Boschitsch and Quackenbush^[1] with an Euler solver including a deforming mesh in the CFD method. However, such a technique is very heavy to implement and not realistic yet to simulate the viscous flows which occur on the rotor. Therefore, researchers have first considered indirect coupling approaches which are easier to manage.

A well-known method to compute blades dynamic response with 3D unsteady transonic aerodynamic effects is a coupling method first developed by Tung et al^[2]. Aerodynamic coefficients, either only the lift coefficient C_l or both the lift and pitching moment coefficients C_l and C_m provided by the CFD solution are introduced in the dynamics code to compute a new rotor trim configuration including blade dynamics. This so-called weak coupling procedure was widely applied by several researchers between dynamics codes using either a finite element approach^{[3],[4],[5]} or a linear elastic beam model^{[6],[7],[8],[9]}, and CFD codes which generally solve the Full-Potential^{[4],[7],[8]} or the Small Disturbances^{[3],[5],[6]} equations. Usually, rigid motion and elastic deformations are transmitted to the CFD code by the blade sections angles-of-attack which are computed by the structure code. However, the way data is exchanged between the dynamics and the

aerodynamics plays an important role in the efficiency of the coupling.

In references [3] to [9], several analyses show that, although an iterative coupling procedure between a rotor dynamics code and a CFD code allows to account for transonic flows and 3D effects in the trim computation, airloads prediction and dynamic blade response are not always efficiently improved. Indeed, according to references [7] and [9], conveying correctly the unsteady blade motion from the dynamics code to the CFD code is essential to accurately compute unsteady 3D aerodynamic coefficients on the blade surface. Furthermore, references [3], [5] and [8] show that introducing three-dimensional pitching moment effects in the dynamics computation has a strong influence on the whole solution and, in particular, the torsion angle prediction near the blade tip is in better agreement with experiment. Finally, it was also pointed out in references [3] and [5] that the rotor wake plays a dominant role in the coupling procedure results and, essentially for low-speed flight cases, it improves the rotor loads correlation with experiment.

This paper proposes to couple a CFD code solving the Euler equations and a dynamics code using a modal approach. To account for the unsteady blade motion in the Euler computation, a moving grid strategy is applied. Then, the 3D lift force, the pitching moment and also the drag force are provided to the rotor trim computation. Results from this coupling procedure are presented for a high-speed flight case ($\mu = 0.4$) on a rectangular blade (7A rotor) or a parabolic-tip blade (7AD rotor). The computed results are correlated with well-documented experimental data which was obtained in S1 Modane^[10] during the 11th test campaign with the 7A and 7AD rotors. Among the data available, one can mention more particularly 116 unsteady pressure transducers, 30 strain gauges, the pitch, flap and lag angles, the forces and moments, and the rotor torque. In this paper, only periodic flight conditions are considered (steady forward flight).

The dynamics code HOST

The HOST code (Helicopter Overall Simulation Tool)^{[11],[12]} was developed by Eurocopter France in order to simulate and analyze the behavior of a complete helicopter or of an isolated rotor. Different kinds of flight conditions can be simulated: steady flight conditions (forward flight, descent, hover,...) which make the assumption of a periodic solution, or maneuvering flight conditions which makes it necessary to compute the solution step by step using a time-marching procedure.

In the present work, HOST is used as a typical rotor dynamics code which provides the trim between the elastic, inertial and aerodynamic loads for an isolated rotor. The blade is assumed to be a linear elastic beam discretized into rigid blade elements linked together by fictive articulations. To compute the dynamic response and elastic deformations in flap, lag and torsion, the Lagrange equations (1) are solved:

$$\frac{d}{dt} \left(\frac{\partial T}{\partial \dot{q}_i} \right) - \frac{\partial T}{\partial q_i} + \frac{\partial U}{\partial q_i} = Q_i \quad (1)$$

where T is the kinetic energy, U the elastic energy, Q_i the generalized loads and q_i the generalized coordinates. In order to reduce the computation time, the unknowns are decomposed as an eigenmodes combination written in the rotating frame. Then, any degree of freedom $h(r, \psi)$ can be written according to relation (2):

$$h(r, \psi) = \sum_{i=1}^{n \text{ modes}} q_i(\psi) \cdot \bar{h}_i(r) \quad (2)$$

where q_i are again the generalized coordinates, depending on the azimuth angle ψ , and \bar{h}_i are the modal shapes, depending on the blade radial position r .

The aerodynamic model used in HOST is based on the lifting line theory. For each blade element, the local Mach number and angle of attack including downwash effects are calculated. Thus, corresponding aerodynamic coefficients C_l , C_m and C_d are directly read in experimental quasi-steady 2D airfoil tables. The airfoil data are then corrected for taking into account the influence of transonic zones, dynamic stall and Reynolds effects. Curvature and sweep corrections are also applied to improve the aerodynamic model. Unsteady effects, predicted by the Theodorsen theory, can also be added on the pitching moment coefficient.

When the trim computation is applied on an isolated rotor, the induced velocities distribution in the spanwise direction can be computed by using either the semi-empirical formulation of Meijer-Drees or by coupling with the rotor wake model METAR^[13]. The Meijer Drees induced velocities are given by the following equation (3):

$$V_{iMD} = V_{im} + \frac{r}{R} V_{ic} \cos \psi - \frac{r}{R} V_{is} \sin \psi \quad (3)$$

where V_{im} , V_{ic} and V_{is} are functions of the global rotor thrust for a given advance ratio and rotating speed of the rotor. The rotor wake model METAR

uses a lattice of straight-line vortex segments, and the induced velocities are computed with the Biot & Savart formula. The wake geometry is prescribed to a helical shape, which depends on the rotor trim conditions. A coupling between the dynamics computation and the METAR model is made until convergence is obtained on the induced velocities.

Finally, the HOST code, used as a rotor dynamics code to predict the rotor trim for a given flight condition, computes the generalized coordinates q_i of the structure and then, by combination with the corresponding modal shapes, it predicts the dynamic response and deformations of the blades in flap, lag and torsion.

The aerodynamic code WAVES

The WAVES code (Without Artificial Viscosity Euler Solver)^[14], developed at ONERA, solves the unsteady three-dimensional Euler equations written in the integral conservation law form. Equations are expressed in the absolute frame linked to the helicopter in order to avoid source terms in the formulation. The numerical scheme is based on a finite-volume method, using Lerat's scheme which is an extension of the predictor-corrector scheme of Lax-Wendroff.

The whole multibladed rotor is enclosed in a multi-block structured grid. Each block is generated around a single blade with a C-H structured topology, and has coincident nodes on the upstream and downstream boundaries to be directly connected with the other blocks (see fig. 1 and fig. 2 for the 4-bladed 7A Rotor). A moving grid approach is then applied to this multi-block mesh to take into account the blades motion in the computation. In its "rigid blade" version, WAVES uses rigid angles provided by the rotor dynamics code HOST to compute a new mesh at each azimuth angle. The modified blade is built by dividing each block into three sub-domains. An inner domain surrounds directly the blade and moves rigidly with it. An outer domain is fixed in order to ensure the connection between two adjacent blocks. Then, an intermediate domain is deformed by keeping the C-H topology and connections with the inner and outer sub-blocks. (see fig. 3).

This moving grid approach was improved by introducing blades elasticity in the computation^[15]. Therefore, the mesh is distorted at each blade radial section, where the deformations in flap, lag and torsional angles are given by the linear combination of the generalized coordinates and modal shapes computed previously by HOST. As a result, the blade rigid motion only appears as a particular case

where only the lower frequency modes are activated.

Finally, WAVES predicts the aerodynamic coefficients C_l , C_m and C_d at each section and for each azimuth by integrating the pressure distributions. This means that no viscous effect is taken into account by the 3D unsteady aerodynamics.

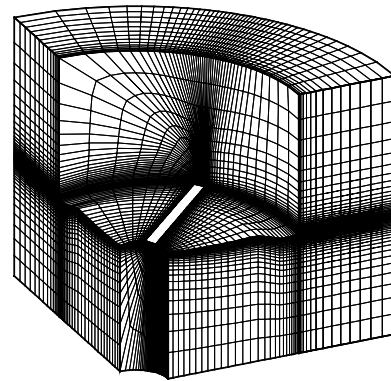


fig. 1 – Mesh block around one blade

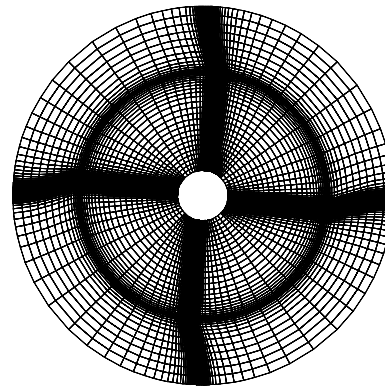


fig. 2 – Multibladed mesh

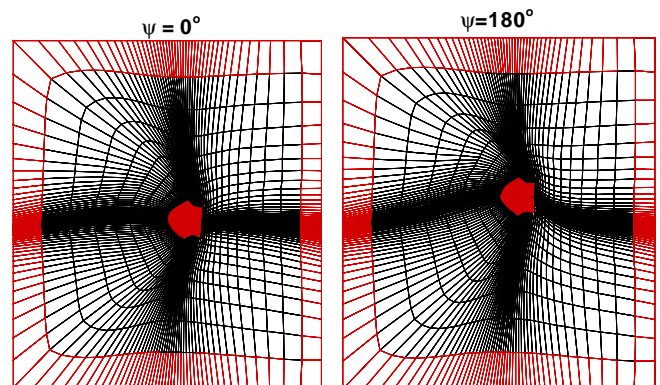


fig. 3 – Deforming mesh strategy

The coupling procedure

The iterative coupling scheme developed between HOST and WAVES is based on the method used in [7], [8] and [9] to couple Full-Potential codes with rotor dynamics codes. Since HOST iteratively computes the global rotor trim for a given forward flight condition, it needs to update the aerodynamic loads in the trim loop by using the 2D airfoil tables. Consequently, it would be impractical to use directly the 3D airloads in the trim computation without increasing considerably the computing time. Therefore, the 3D unsteady aerodynamic effects are introduced in the dynamic computation by correcting the 2D quasi-steady airloads. Finally, the following iterative procedure is applied between HOST and WAVES:

1) HOST computes the blade dynamic response and deformations by trimming the rotor with the 2D aerodynamics provided by airfoil tables. The modal shapes being determined previously, the generalized coordinates contain all the information concerning the rigid and elastic blade motion.

2) The generalized coordinates are provided to WAVES which computes a new grid deformation law along one blade revolution.

3) The CFD computation determines the 3D lift F_z^{3D} , drag F_x^{3D} and pitching moment M_y^{3D} at each radial section and azimuth angle from aerodynamic coefficients distributions on the blade surface.

4) In the HOST code, a correction on the aerodynamic loads is calculated according to the relation (4):

$$\Delta F_z = F_z^{3D} - F_z^{2D} \quad (4)$$

where F_z^{2D} is the lift force computed from the lift coefficient read in airfoil tables.

5) Then, HOST trims again the rotor with the corrected aerodynamic loads, noted F_z^{HOST} , given at each radial sections and azimuth angle by the relation (5):

$$F_z^{HOST} = F_z^{2D} + \Delta F_z \quad (5)$$

A new dynamic and elastic blade response is thus determined by computing new generalized coordinates.

6) Steps 2 to 5 are then repeated until convergence is achieved.

Finally, no relaxation is used in the coupling procedure. Several coupling schemes have been implemented and tested in this study: either the 3D lift, or both the 3D lift and pitching moment, or also

the 3D lift, pitching moment and drag are simultaneously coupled.

The coupled solution is converged if global coefficients (such as the collective pitch, the cyclic pitch, the rotor shaft angle or the torque coefficient), local aerodynamics loads, or local elastic deformations (such as torsion angle) are "quite similar" from one coupling iteration to the following.

Results and Discussion

In this section, the coupling procedure described above is validated for the following forward flight condition:

$\mu=0.4$; $M_{\Omega R}=0.646$; $200 C_z/\sigma=12.5$; $C_x S/S\sigma=0.1$ and the Modane law (i.e. $\beta_{1c} = \theta_{1s}$ and $\beta_{1s} = 0$) for trimming.

The solutions are presented first for the 7A rotor equipped with rectangular blades and then, for 7AD rotor with parabolic blade tips.

7A ROTOR

Effect of F_z coupling and of F_z and M_y coupling:

The objective of this section is to investigate the standard coupling schemes which have been used up to now in this field. The results presented in fig. 4 to fig. 7 come from a coupled computation between HOST and WAVES in which HOST used the rotor wake model METAR to compute the induced inflow.

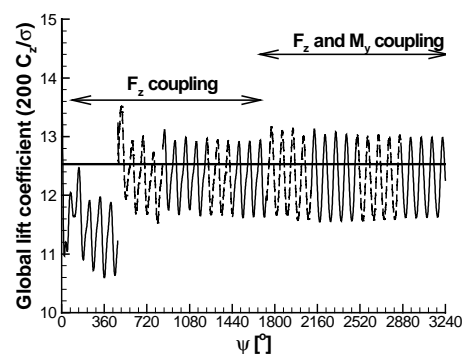


fig. 4 – Effect of F_z and M_y coupling on the global lift coefficient computed by the CFD code WAVES

Fig. 4 shows the evolution of the global rotor lift coefficient (contribution of the 4 blades) predicted by the WAVES computation after each

coupling iteration. Each element of the curve represents a coupling iteration and therefore roughly a blade revolution. The strong 4 per-rev. lift variation can be clearly noticed: this is due to the 4-bladed configuration. The nominal experimental value is represented by the straight line. The first coupling iteration uses a trim condition which comes from a pure 2D aerodynamic computation and the CFD solution thus provides a mean lift coefficient different from the nominal one : 11.2 instead of 12.5. As soon as the HOST trim uses the 3D corrections, this lift value becomes much closer to the desired one and the following iterations do not bring a significant improvement on this aspect. However, the M_y coupling tends to increase slightly the 4 per-rev. fluctuation of the lift around its mean value.

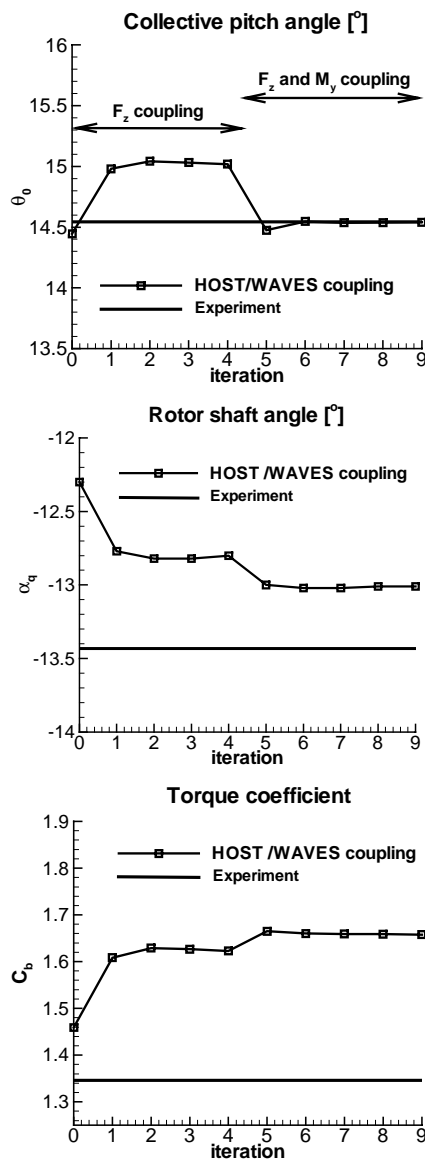


fig. 5 – Effect of F_z and M_y coupling on trim parameters

The convergence of the global coefficients (collective pitch, rotor shaft angle and torque coefficient) versus the coupling iterations is shown in fig. 5. The convergence is fast for all these quantities and a jump appears both when the coupling is applied and when the computation is switched from “ F_z coupling” to “ F_z and M_y coupling”. The experimental values are also shown as straight lines. The prediction of the collective pitch and rotor shaft angles is improved by the converged solution compared with experiment, while the torque coefficient prediction is spoiled by the coupling. This point will be discussed below.

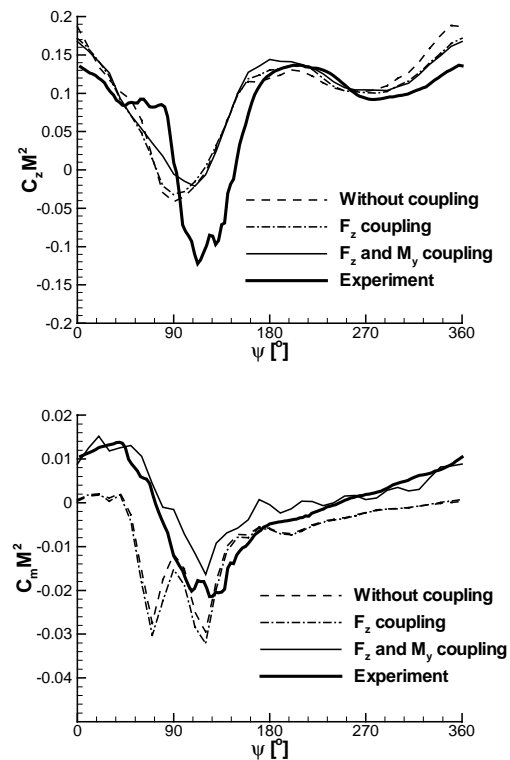


fig. 6 – $C_z M^2$ and $C_m M^2$ distributions near the blade tip ($r/R=0.975$): comparison of experiment, 2D calculation, F_z coupling and F_z and M_y coupling results.

In fig. 6, the $C_z M^2$ and $C_m M^2$ values are plotted after convergence for both the “ F_z ” coupling and the “ F_z and M_y ” coupling computations. A comparison is made with experiment and with the 2D solution. The influence of 3D effects on $C_z M^2$ prediction is weak compared to the discrepancy between the 2D computation and the experiment. On the contrary, the influence of coupling on the moment coefficient is quite large especially on the advancing blade side. However this benefit is only obtained when a “ $F_z + M_y$ ” coupling is applied. As a matter of fact, the “ F_z ” coupling modifies the rotor trim and more especially the pitch angle, but the aerodynamic loads remain close to the values coming from a 2D aerodynamics. On the other

hand, the “ $F_z + M_y$ ” coupling modifies the torsional deflection of the blades which results in a quite different trim condition. This is confirmed by fig. 7 where the evolution of the torsion angle is represented versus azimuth angle at the blade tip. It is noteworthy that the “ $F_z + M_y$ ” coupling greatly improves the prediction of the low frequency component of the blade torsion at the tip. However, this figure also shows the lack of the 5 per-rev. high frequency component of torsion.

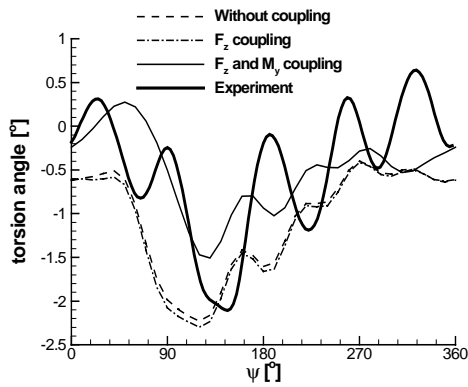


fig. 7 – Torsion angle distribution near the blade tip ($r/R=0.975$): comparison of experiment, 2D calculation, F_z coupling and F_z and M_y coupling results.

Influence of induced velocities model:

One of the aim of the dynamics/aerodynamics coupling is to replace the simplified aerodynamic model used in the dynamics code by the 3D unsteady aerodynamics given by the CFD solution. Indeed, at convergence, the coupled solution should be independent on the simplified aerodynamics used in the dynamics code. In order to check this, the same computation presented above was run using the analytical Meijer Drees inflow model in HOST.

As shown by fig. 8, this independence on the inflow model is not obtained neither for the “ F_z ” coupling nor for the “ $F_z + M_y$ ” coupling. All the trim conditions are significantly different between the two inflow models.

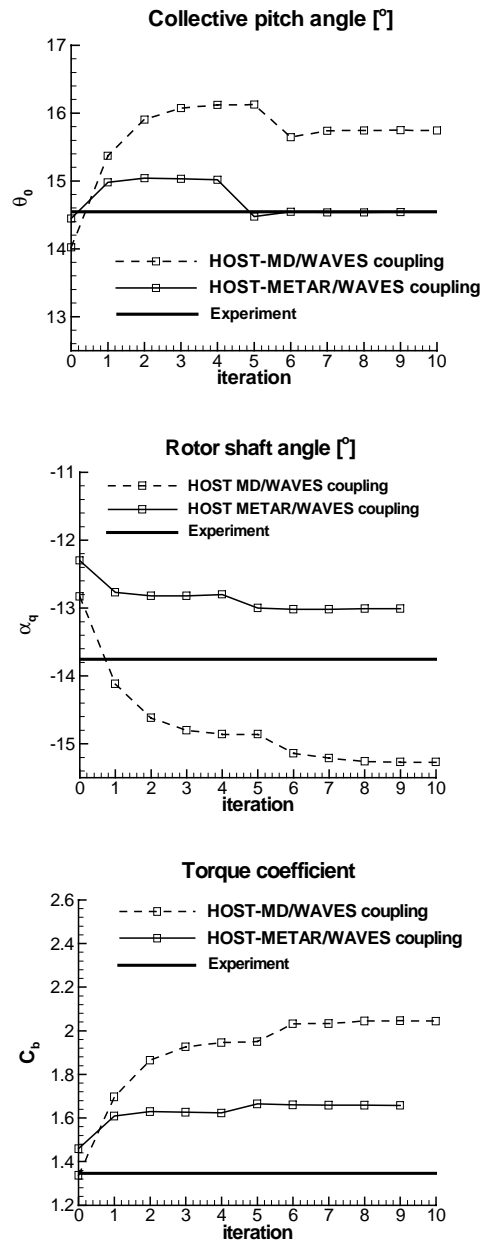


fig. 8 – Comparison of trim parameters solutions for a HOST-MeijerDrees/WAVES and for a HOST-METAR/WAVES F_z and M_y coupling computations.

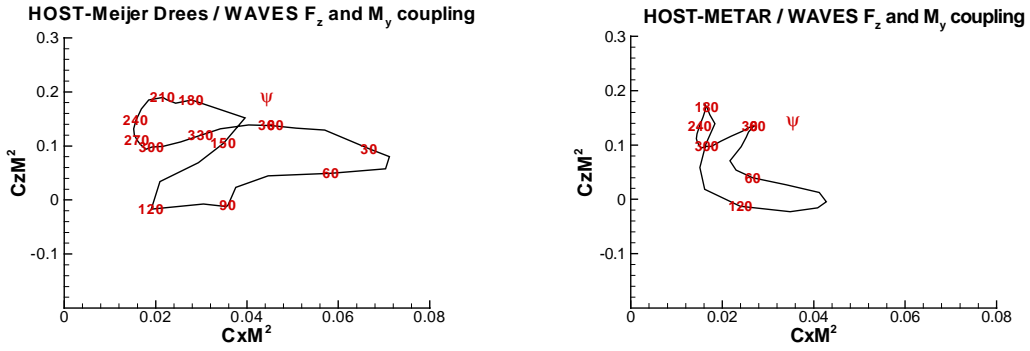


fig. 9 - C_zM^2 versus C_xM^2 near the blade tip, for a HOST-Meijer Drees/WAVES and for a HOST-METAR/WAVES F_z and M_y coupling computation.

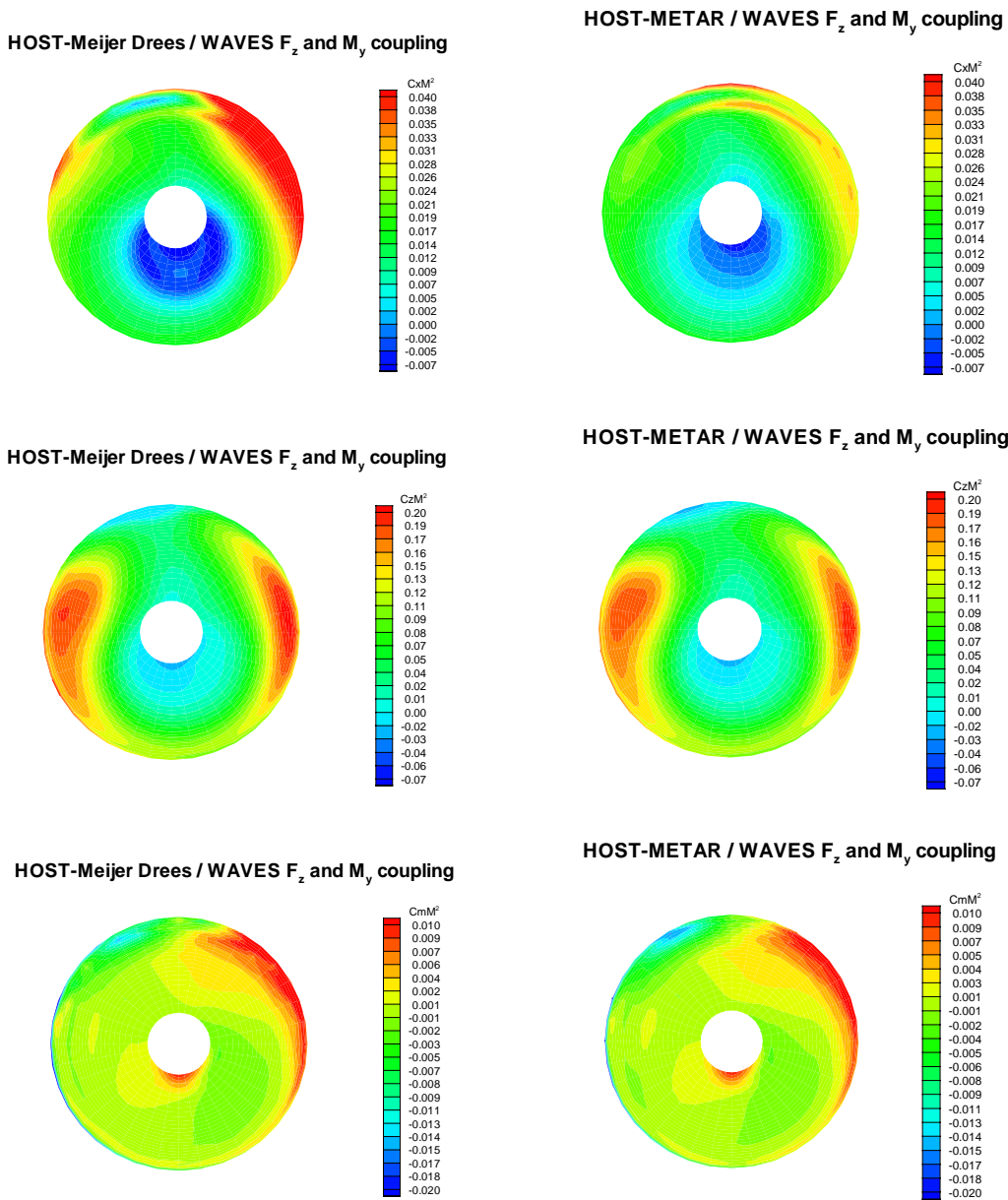


fig. 10 - C_xM^2 , C_zM^2 and C_mM^2 repartitions on the rotor disk, for a HOST-Meijer Drees/WAVES (left) and for a HOST-METAR/WAVES (right) F_z and M_y coupling computation.

In fact, the problem arises from the 3D corrections introduced, which are inconsistent with the aerodynamic characteristics of the blades airfoils. Indeed, introducing lift and pitching moment corrections without modifying the drag is equivalent to modify the airfoil polars. This effect is magnified when the solutions using the analytical model of Meijer Drees and the METAR vortex wake model are compared because the incidences at the blade tip are quite different, the METAR model giving an incidence angle close to zero. This is clearly noticeable in fig. 9 which plots the working conditions (lift vs. drag) of a blade section at the tip along a blade revolution. It shows that, although the lift variation is very similar between the Meijer Drees and the METAR coupled solutions, the former one gives a much larger peak to peak variation for the drag evolution versus azimuth. Indeed, the high angles-of-attack at the blade tip provide strong shock waves when the Meijer Drees model is used. This phenomenon is not only local but, as shown by fig. 10, the drag distribution over the rotor disk significantly differs between the Meijer Drees and METAR solutions, while the lift and moment distributions are very similar. This shows the necessity to introduce as well an F_x correction in the coupling process. This should give working conditions for the blade sections which are independent on the inflow model used, the actual wake influence being given by the CFD solution. Furthermore, one can expect to improve (at least modify) the correlation with experiment for the torque coefficient.

F_z , M_y and F_x coupling:

The basic idea of adding a F_x coupling is, as for the F_z and M_y coupling, to correct the inviscid part of these quantities with a 3D unsteady component. However, one can notice that, in the coupling procedure, the corrective term $\Delta F_x = F_x^{3D} - F_x^{2D}$ represents the subtraction between a non viscous quantity and a viscous one. Then, for the drag, this correction mainly corresponds to a correction of the wave drag created by the shocks which appear on the blade.

In practice, the coupling is made simultaneously for the three quantities F_z , F_x and M_y . As shown by fig. 11 this coupling converges again very rapidly. Furthermore, the converged solutions are quite close whatever the induced velocities model used. Finally, the prediction of the torque coefficient is improved by the coupling contrary to what was observed without F_x coupling.

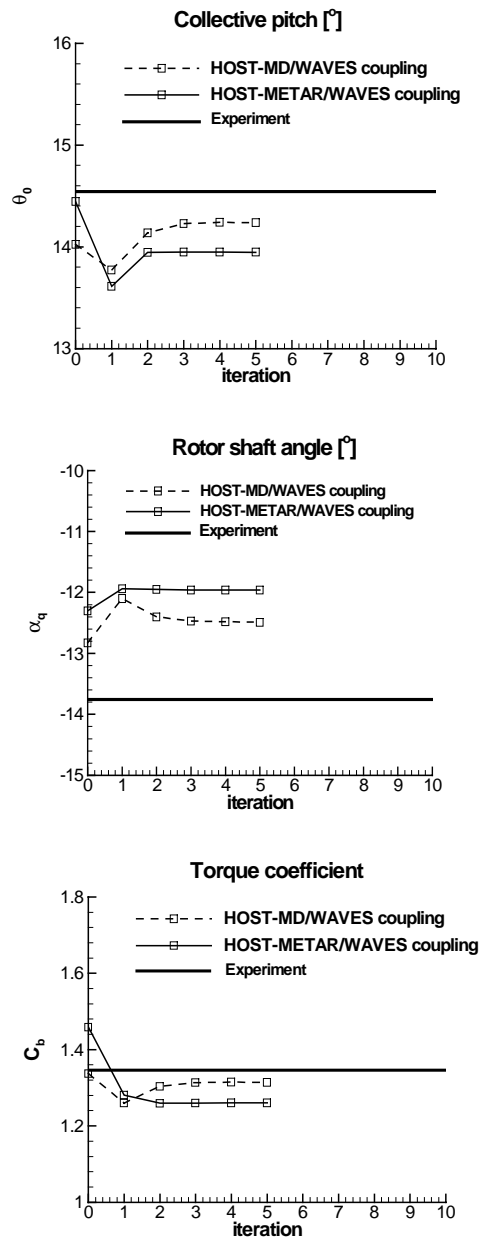


fig. 11 - Comparison of trim parameters solutions for a HOST-MeijerDrees/WAVES and for a HOST-METAR/WAVES F_z , F_x and M_y coupling computations

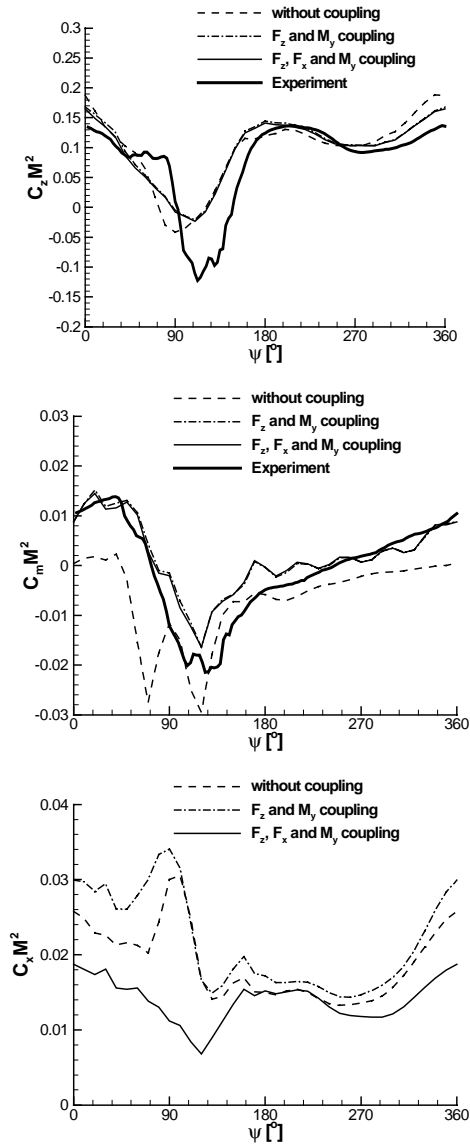


fig. 12 - $C_z M^2$, $C_m M^2$ and $C_x M^2$ distributions near the blade tip ($r/R=0.975$): comparison of experiment, 2D calculation, F_z and M_y coupling and F_z , F_x and M_y coupling results.

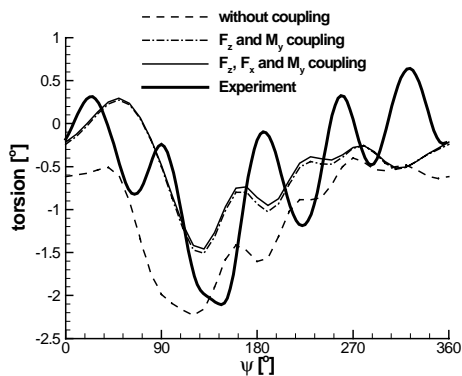


fig. 13 - Torsion angle distribution near the blade tip ($r/R=0.975$): comparison of experiment, 2D calculation, F_z and M_y coupling and F_z , F_x and M_y coupling results.

The additional F_x coupling has almost no influence on the $C_z M^2$ and $C_m M^2$ predictions as shown by fig. 12, which proves that a significant progress is still necessary to predict correctly the lift evolution on the advancing blade side. Furthermore, the $C_x M^2$ is strongly modified by the F_x coupling on the advancing side which tends to confirm that the 3D correction is most important for the flow regions where compressibility is predominant. As expected, the torsional deformation at the blade tip is hardly affected by the F_x coupling and its high frequency component is still largely under-estimated, which probably explains the poor lift prediction at the tip (see fig. 13).

Finally, as shown by fig. 14 and fig. 15, the rotor aerodynamics after convergence is very similar between the Meijer-Drees and METAR solutions, which confirms that the aerodynamic loads and moments in the trimmed solution are provided by the CFD analysis.

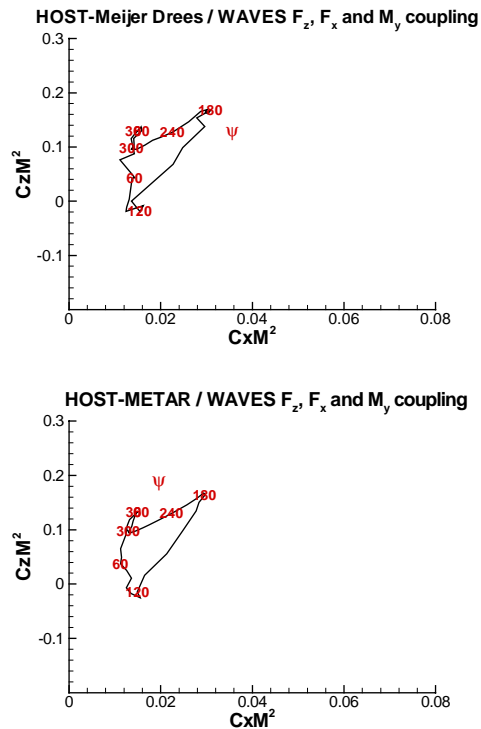
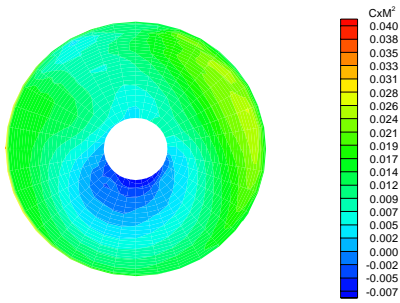


fig. 14 - $C_z M^2$ versus $C_x M^2$ near the blade tip, for a HOST-Meijer Drees/WAVES and for a HOST-METAR/WAVES F_z , F_x and M_y coupling computation.

HOST-Meijer Drees / WAVES F_z , F_x and M_y coupling



HOST-METAR / WAVES F_z , F_x and M_y coupling

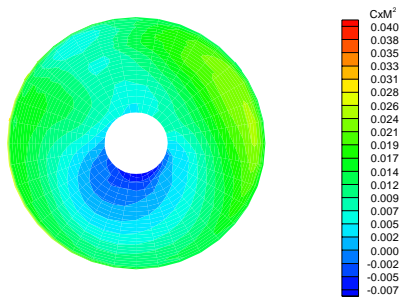


fig. 15 - $C_x M^2$ repartition on the rotor disk, for a HOST-Meijer Drees/WAVES and for a HOST-METAR/WAVES F_z , F_x and M_y coupling computation.

7AD ROTOR

To further test the present approach, the coupled F_z , F_x and M_y scheme was applied to a rotor equipped with non rectangular blades for the same flight condition: the 7AD rotor with its parabolic SPP8 tips. In this coupling computation, HOST uses a curvature correction to account for the sweep influence in the dynamics computation.

As shown by fig. 16, the trim parameters converge again within a few iterations and the strong variation appearing as soon as the F_z , F_x and M_y coupling procedure is applied leads to an almost constant solution then, as was already found for the 7A rotor. However, the converged parameters are more distant from the experimental values than for the 7A.

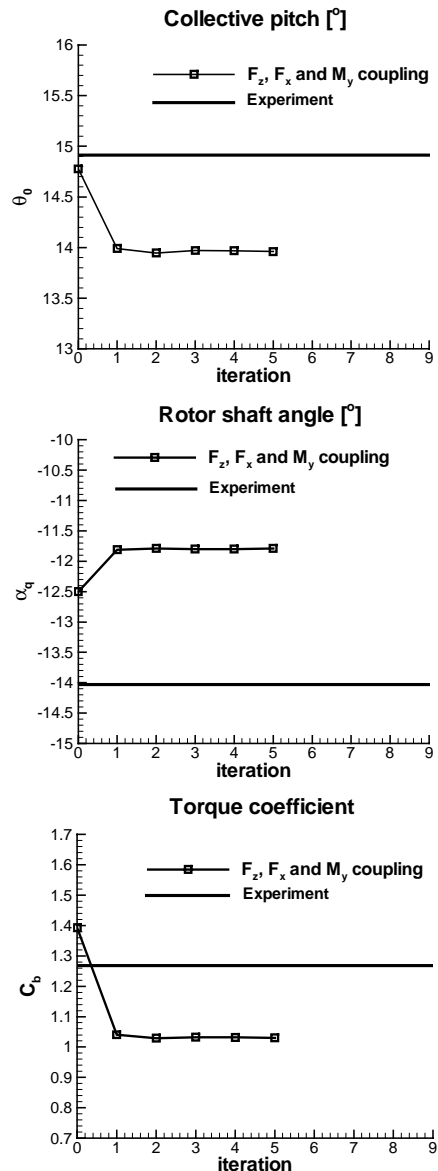


fig. 16 - Effect of F_z , F_x and M_y coupling on trim parameters for the 7AD rotor.

The influence of F_z , F_x and M_y coupling is also noticeable on the lift and pitching moment distribution according to fig. 17. Indeed, a larger influence of the coupling is found on the $C_z M^2$ prediction than for the rectangular blade. Unfortunately, the correlation with experiment of the coupled solution is worse than that of the isolated HOST computation. Although this result may be disappointing, it shows that the curvature corrections introduced in the HOST lifting line model are efficient. As for the 7A rotor study, the $C_m M^2$ distribution versus azimuth is also in better agreement with experiment, in particular on the advancing blade side, when the coupling procedure is applied. However, a phase shift can be noticed between the coupled solution and experiment which didn't appear in the 7A rotor $C_m M^2$ prediction. This shift may explain the worse correlation observed on

the lift. Finally, the coupling procedure improves as well the prediction of torsional deformation at the blade tip and high torsional frequencies are again under-estimated (see fig. 18).

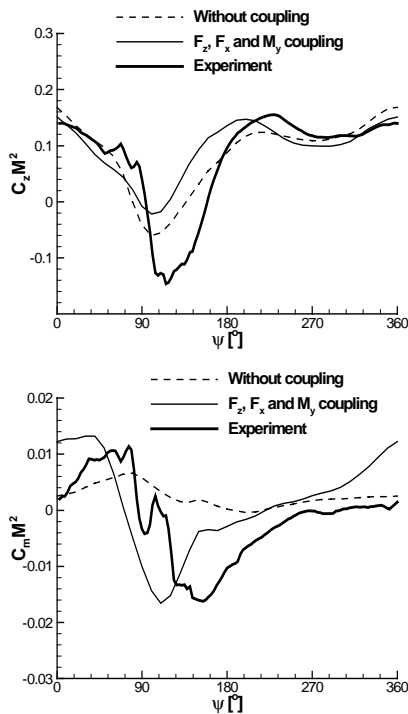


fig. 17 – $C_z M^2$ and $C_m M^2$ distributions near the blade tip ($r/R=0.975$): comparison of experiment, 2D calculation and F_z , F_x and M_y coupling results.

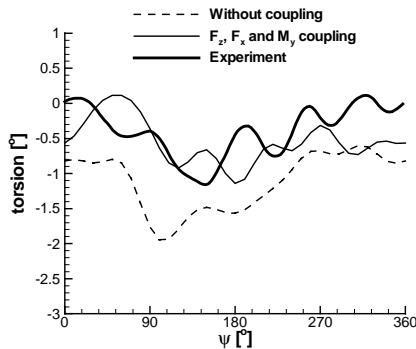


fig. 18 – Torsion angle distribution near the blade tip ($r/R=0.975$): comparison of experiment, 2D calculation, F_z , F_x and M_y coupling results.

Conclusions

A weak coupling procedure between the Euler aerodynamic solver WAVES and the HOST dynamics code has been developed for computing an isolated rotor in steady forward flight conditions. The WAVES solution computes the 3D unsteady inviscid aerodynamic field around the flexible rotor

using a multi-block grid made of deforming meshes around each rotor blade with coincident interfaces. The blade motion and deformation is given by the HOST trimmed solution which is introduced in WAVES by using the general coordinates and the mode shapes of the blades in order to be able to prescribe the full rotor dynamics in the aerodynamic solution. The HOST code uses the beam theory and a simplified aerodynamic model to compute the rotor trim, and it receives the 3D forces and moments around the blades from WAVES in order to correct the simplified aerodynamics in the trim process. An iterative coupling between the dynamics and the CFD solution allows to converge rapidly in less than 5 iterations.

The work presented in this paper shows that the converged solution is independent on the simplified aerodynamic model used in HOST, and in particular on the induced velocities model, only if a simultaneous lift F_z , drag F_x and pitching moment M_y coupling is applied. Indeed, when this condition is not met, e.g. by coupling only on the F_z or F_z and M_y components, the airfoil polars used in the trim computation may be inconsistent with the actual characteristics of the airfoils which equip the blade.

Comparison with experiment shows that the coupling always improves significantly the prediction of pitching moment and torsion angle at the blade tip. However, the high frequency component of torsion is not accurately captured, which does not allow to improve the prediction of lift. As a result, the global coefficients are generally not better predicted than with a simplified aerodynamics. This shows the complexity of the rotor trim problem which is dependent on a large number of parameters.

In order to improve this correlation with experiment, two ways of research will have to be explored. The first one consists in accounting for the viscous effects in the CFD solution by using a Navier-Stokes method, so that the full 3D aerodynamic field is used in the trim computation. The second point to investigate is the coupling process itself. Instead of computing the blade dynamics and aerodynamics separately and of coupling them over each blade revolution, the direct solution of dynamics and aerodynamics simultaneously at each blade azimuth has to be investigated. This “strong coupling” approach should better represent the couplings which occur between the soft blade and the actual unsteady aerodynamic field.

References

- [1] Boschitsch, A.H., Quackenbush, T.R., “*Prediction of Rotor Aeroelastic Response Using a New Coupling Scheme*”, AIAA, 25th Fluid Dynamics Conference, Colorado Springs, Colorado, June 1994.
- [2] Tung, C., Caradonna, F.X., Johnson, W., “*The Prediction of Transonic Flow on an Advancing Rotor*”, Journal of the American Helicopter Society, Vol. 31, No 3, July 1986, pp 4-9.
- [3] Kim, K.C., Chopra, I., “*Effects of Three-Dimensional Aerodynamics on Blade Response and Loads*”, AIAA/ASME/ASCE/AHS/ASC 30st Structures, Structural Dynamics and Materials Conference, Mobile, Alabama, April 1989.
- [4] Gea, L-M, Chow, C-Y, Chang, I-C, “*Transonic Aeroelasticity Analysis for Rotor Blades*”, AIAA, 7th Applied Aerodynamics Conference, Seattle, July 31-August 2, 1989.
- [5] Desopper, A., Chopra, I., Kim, K.C., “*Dynamic Blade Response Calculations using Improved Aerodynamic Modeling*”, National Specialists’ Meeting on Aerodynamics and Acoustics, Fort Worth, Texas, February 1987.
- [6] Tran, C.T, Desopper, A., “*An iteration Technique Coupling 3-D Transonic Perturbation Aerodynamic Theory and Rotor Dynamics in Forward Flight*”, 14th European Rotorcraft Forum, Milano, Italy, September 1987.
- [7] Strawn, R.C., Bridgeman, J.O., “*An improved Three-Dimensional Aerodynamics Model for Helicopter Airloads Prediction*”, 29th Aerospace Sciences Meeting, Reno, Nevada, January 1991.
- [8] Beaumier, P., “*A Coupling Procedure between a Rotor Dynamics Code and a 3D Unsteady Full Potential Code*”, American Helicopter Society Aeromechanics Specialists Conference, San Francisco, California, January 1994.
- [9] Strawn, R.C., Desopper, A., Miller, J., Jones, A., “*Correlation of Puma Airloads Evaluation of CFD Prediction Methods*”, 14th European Rotorcraft Forum, Milano, Italy, September 1987.
- [10] Crozier, P., “*Recent improvements in rotor testing capabilities in the ONERA SIMA Wind Tunnel*”, 20th European Rotorcraft Forum, Amsterdam, The Netherlands, October 1994.
- [11] Benoit, B., Gaulene, P., Martin, P., “*HOST-Helicopter Overall Simulation Tool*”, User Manual, Eurocopter France, Marignane, 1997.
- [12] Benoit, B., Dequin, A.-M., Kampa, K., Grunhagen, W., Basset, P.-M., Gimonet, B., “*HOST, A General Helicopter Simulation Tool for Germany and France*”, American Helicopter Society, 56th Annual Forum, Virginia Beach, Virginia, May 2000.
- [13] Arnaud, G., Beaumier, P., “*Validation of R85/METAR on the Puma RAE Flight Tests*”, 18th European Rotorcraft Forum, Avignon, France, September 1992.
- [14] Boniface, J.C., “*Calcul d’écoulements compressibles autour de rotors d’hélicoptères en vol stationnaire ou en vol d’avancement par résolution des équations d’Euler*”, Ph.D. Thesis, Ecole Nationale Supérieure des Arts et Métiers, December 1995.
- [15] Beaumier, P., Reboul, G., “*Application d’un code Euler pour le calcul du rotor d’hélicoptère en vol d’avancement*”, RTS 216/1369 DAAP/Y, July 1998.